

The nature and extent of the Mesoproterozoic Picuris orogeny in Colorado

This is a preliminary GSA Guidebook by Kuiper, et. al. May 9, 2022

For a Colorado Scientific Society field trip on June 7, 2022

Yvette D. Kuiper

Department of Geology & Geological Engineering, Colorado School of Mines, Golden, Colorado 80401, USA

Ruth F. Aronoff

Department of Earth, Environmental & Sustainability Sciences, Furman University, Greenville, South Carolina

29613, USA

Christopher G. Daniel

Department of Geology & Environmental Geosciences, Bucknell University, Lewisburg, Pennsylvania 17837, USA

Madison Bzdok

Department of Geology & Geological Engineering, Colorado School of Mines, Golden, Colorado 80401, USA

(currently at Newmont)

ABSTRACT

The Mesoproterozoic is a controversial time within the Earth's history, and is characterized by high T/P ratios in metamorphic rocks, a large volume of extensional plutons, very few economic mineral deposits, and (arguably) a slow-down in plate tectonic processes. In Laurentia, ~1.48–1.35 Ga is well known as a time of ferroan magmatism. Recently, a ~1.50–1.35 Ga orogenic belt was proposed that spanned Laurentia from present-day eastern Canada to the southwestern United States. Unlike the preceding Paleoproterozoic Yavapai/Mazatzal orogenies and the subsequent late Mesoproterozoic Grenville orogeny, the early-mid-Mesoproterozoic Picuris orogeny in the southwestern U.S. was relatively unrecognized until about two decades ago, when geochronology data became more abundant. In multiple study areas of Arizona and New Mexico, deposition, metamorphism and deformation previously ascribed to the Yavapai/Mazatzal orogenies proved to be part of the ~1.4 Ga Picuris orogeny. In Colorado, the nature and extent of the Picuris orogeny is poorly understood. On this trip, we discuss new

26 evidence for the Picuris orogeny in the central Colorado Front Range, from Black Hawk in the
27 central Colorado Front Range to the Wet Mountains, Colorado. We will discuss how the Picuris
28 orogeny reactivated or overprinted earlier structures, and perhaps controlled the location of
29 structures associated with Cambrian rifting, the Cretaceous-Paleogene Laramide orogeny, and
30 the Rio Grande Rift, and associated mineralization. We will also discuss what made the Picuris
31 orogeny, and the Mesoproterozoic unique within the Earth's history.

32

33 **INTRODUCTION**

34 Globally, the Mesoproterozoic is characterized by a number of anomalies compared with
35 pre- and post-Mesoproterozoic periods. These include a decrease in the number of passive
36 margins, detrital zircons, greenstone-belt collisions, eclogites, granulites, carbonatites, and
37 orogenic gold (Bradley et al., 2011), higher T/P ratios of metamorphic rocks, and more juvenile
38 and thinned crust (Brown et al., 2020; Spencer et al., 2021). The reason for these anomalies is
39 not known, but was interpreted previously as a slow-down of tectonic processes during the
40 Columbia/Nuna-Rodinia supercontinent transition, or as a period of plate tectonics characterized
41 by hot, thin, and low orogens (Spencer et al., 2021, and references therein). The Mesoproterozoic
42 Picuris orogen of the southwestern U.S. (Daniel et al., 2013, 2022a,b), provides an opportunity to
43 investigate and discuss these processes. The focus of this field trip is to examine the nature and
44 extent of the Picuris orogen in the Colorado Front Range. We will also discuss how it reactivates
45 earlier Paleoproterozoic structures and may control later Phanerozoic structures.

46 Proterozoic rocks of the southwestern U.S. (Figs. 1, 2) preserve a record of significant
47 Paleoproterozoic crustal growth southward from the Archean Wyoming Province (present day
48 coordinates), and experienced multiple orogenic events including the Paleoproterozoic Yavapai

49 and Mazatzal orogenies (Whitmeyer and Karlstrom, 2007; Jones et al., 2009; Holland et al.,
50 2020), and the Mesoproterozoic Picuris orogeny (Daniel et al., 2013). Voluminous ~1.48–1.35
51 Ga granitic magmatic rocks are also associated with the Mesoproterozoic, and make up about
52 25–30% of the exposed Proterozoic rock in the southwestern U.S. The occurrence of significant
53 ferroan, granitic magmatic rocks, typically attributed to an extensional environment (Anderson
54 and Morrison, 2005; Frost and Frost, 2022), and crustal thickening associated with the
55 contractional Picuris orogeny overlap in time and space and present an intriguing
56 contradiction with respect to the tectonic setting of Laurentia during the Mesoproterozoic (Daniel
57 et al., 2022a,b; Frost and Frost, 2022).

58 In Colorado, ~1.4 Ga deformation and metamorphism were previously recognized and
59 interpreted as relatively localized events related to pluton emplacement or as reactivation along
60 Paleoproterozoic foliations and shear zones (Fig. 2; Pedrick et al., 1998; Selverstone et al., 2000;
61 Shaw et al., 2001; McCoy et al., 2005, Shaw and Allen, 2007; Allen and Shaw, 2011; Lytle,
62 2016). This field trip includes visits to exposures in the central Colorado Front Range and in the
63 Wet Mountains (Fig. 2) to examine new evidence for ~1.4 Ga metamorphism and deformation,
64 and discuss how to separate the Mesoproterozoic from older Paleoproterozoic events. We will
65 discuss the larger scale nature of deformation across the southern margin of Laurentia, and how
66 the Picuris Orogen correlates with the Baraboo and Pinware orogens of the midcontinent and
67 eastern Canada, respectively (Fig. 1). We also highlight overprinting Cambrian rift structures and
68 mineralized rocks, and Cretaceous–Paleogene structures and mineralized rocks associated with
69 the Laramide orogeny. We will discuss how and why the Mesoproterozoic Picuris orogeny was
70 different from earlier and later orogenies on Earth and how Proterozoic tectonism may have
71 controlled later structures and mineralization.

72 GSA designated this as a Warren Hamilton field trip, which supports student
73 participation. Warren B. Hamilton (1925–2018) integrated geology and geophysics into large-
74 scale tectonic and planetary-scale syntheses. He was an outside-the-box thinker and always
75 encouraged stimulating and thought-provoking discussion. In that spirit, this field trip will have
76 ‘questions for discussion’ at each stop, where we encourage all to discuss those questions and
77 others that may arise, and particularly include our early-career participants.

78

79 **PROTEROZOIC OROGENIC EVENTS IN COLORADO**

80 **The Yavapai and Mazatzal Orogenies**

81 The Paleoproterozoic Yavapai and Mazatzal orogenies were first defined in Arizona
82 (Karlstrom and Bowring, 1988; Bowring and Karlstrom, 1990) and have subsequently been
83 extended to the NE and across the midcontinent (Whitmeyer and Karlstrom, 2007).
84 Paleoproterozoic amphibolite facies metasedimentary and metaigneous rocks in the Colorado
85 Front Range (e.g., Gable, 2000; Widmann et al., 2000; Kellogg et al., 2008) were interpreted as
86 juvenile arc terranes with associated basins that amalgamated and accreted to the Wyoming
87 Craton part of Laurentia between ~1.8 Ga and ~1.6 Ga (Whitmeyer and Karlstrom, 2007).
88 Alternatively, Jones et al. (2009) and Holland et al. (2020) proposed that the Paleoproterozoic
89 rocks of the southwestern U.S. formed largely within a continental arc setting that experienced
90 alternating periods of slab roll and extension to create back-arc basins that were subsequently
91 closed and inverted by advancement of the subduction zone and compression. In general, two
92 periods of orogenesis including the ~1.72–1.68 Ga Yavapai and ~1.65–1.6 Ga Mazatzal
93 orogenies have been recognized across the southwestern U.S. for more than 35 years, which may
94 or may not have been a continuous period of deformation (Jones and Connelly, 2006; Mahan et

95 al., 2013). The resultant Yavapai crustal province is now a NE-trending zone of predominantly
96 juvenile crust that extends from Arizona to Michigan (Fig. 2; Whitmeyer and Karlstrom, 2007),
97 and forms most of the Proterozoic basement of Colorado. Calc-alkaline plutons intruded the
98 Yavapai basement of Colorado between about ~1.66 Ga and 1.65 Ga. The Mazatzal crustal
99 province extends from Arizona to Quebec and Labrador in Canada (Figs. 1, 2; Whitmeyer and
100 Karlstrom, 2007), and probably includes older Paleoproterozoic crustal material (Holland et al.,
101 2020) Between ~1.60 Ga and ~1.5 Ga Laurentia underwent a period of tectonic quiescence
102 (Whitmeyer and Karlstrom, 2007; Doe et al., 2012; Aronoff, et al., 2016). Interestingly,
103 deformation in the Mazatzal Mountains of Arizona is now known to be ~1.47–1.43 Ga (Doe et
104 al., 2012; Doe and Daniel 2019), the general age of the Picuris orogeny.

105

106 **The Picuris Orogeny**

107 Mesoproterozoic ~1.5–1.45 Ga deposition of siliciclastic sediments in the southwestern
108 U.S. was first reported in the Picuris Mountains, New Mexico (Jones et al., 2011; Fig. 1) and the
109 upper Salt River Canyon, Arizona (Doe et al., 2012; Fig. 1). Additional rocks of this age are
110 known from the Defiance uplift, Four Peaks, and the northern Mazatzal Mountains of Arizona
111 (Doe et al., 2013, Mako et al., 2015; Doe and Daniel, 2019; Figs. 1, 2). These rocks and the
112 underlying Yavapai and Mazatzal basement across much of central and northern New Mexico
113 experienced greenschist to uppermost amphibolite facies metamorphism and deformation
114 between ~1.44 Ga and ~1.37 Ga, including the Tusas and Taos mountains of New Mexico
115 (Pedrick et al., 1998; Kopera, 2003; Fig. 2). Several areas also experienced emplacement of
116 ~1.45–1.40 Ga granitic plutons and preserve contact metamorphic aureoles (Four Peaks, upper
117 Salt River Canyon, southern Picuris Mountains; Fig. 2). The recognition of ~1.50–1.35 Ga

118 deposition, regional metamorphism and deformation, and magmatism led to the proposed Picuris
119 orogeny (Daniel et al., 2013; Aronoff et al., 2016; Bollen et al., 2022).

120 Mesoproterozoic, ~1.43–1.36 Ga metamorphism and deformation is also observed in the
121 Wet Mountains, the Needle Mountains, and the region around the Black Canyon of the
122 Gunnison, southern Colorado, Big Thompson Canyon of central Colorado, (Fig. 2; Shaw et al.,
123 2001; McCoy et al., 2005; Jessup et al., 2006; Jones et al., 2010; Shah and Bell, 2012; Mahan et
124 al., 2013; Lytle, 2016). Recent and ongoing research from the central Front Range of Colorado
125 also indicates Mesoproterozoic deformation, not only reactivation along shear zones, but also
126 pervasive folding (Lytle, 2016; Mahatma, 2019; Powell, 2020; Shockley, 2021). This is further
127 discussed below.

128 The Picuris orogen is part of a larger, trans-Laurentian orogen that include the Baraboo
129 and Pinware orogens of the midcontinent and eastern Canada, respectively (Daniel et al., 2022a,
130 b; Fig. 1), This Pinware-Baraboo-Picuris orogenic belt is attributed to a convergent or
131 accretionary plate margin across the southern margin of Laurentia (present-day coordinates). In
132 eastern Canada, the ~1.51–1.46 Ga Pinware orogeny involved convergence and subduction
133 within the proto-Grenville province in Labrador and eastern Quebec (Tucker and Gower, 1994;
134 Gower and Krogh, 2002; Groulier et al., 2020). Similarly, the midcontinent Baraboo orogeny
135 yielded 1493–1465 Ma muscovite $^{40}\text{Ar}/^{39}\text{Ar}$ ages, and plutons in that same age range (Medaris et
136 al., 2021). The ~1.48–1.35 Ga Picuris orogeny in northern New Mexico involved convergence
137 and possible collision between Laurentia and juvenile crust along the southern margin of
138 Laurentia (Aronoff et. al., 2016). This created shortening and thickening of Paleo- and
139 Mesoproterozoic rocks (Daniel and Pyle, 2006; Daniel et al., 2013; Aronoff et al., 2016; Daniel
140 et al. 2022b).

141 Between ~1.48 Ga and 1.36 Ga, granitoids were emplaced in a broad belt spanning from
142 the southwestern U.S. through the Baltic shield (Fig. 2; Windley, 1993; Karlstrom and
143 Humphreys, 1998; du Bray et al., 2018). These granitoids may be divided into ~1.49–1.41 Ga
144 and ~1.41–1.34 Ga pulses (Whitmeyer and Karlstrom, 2007). They were interpreted as
145 anorogenic (Anderson and Morrison, 2005; Goodge and Vervoort, 2006). However, episodes of
146 significant deformation and metamorphism are now recognized in parts of New Mexico, Arizona
147 and Colorado at these times of pluton emplacements (Nyman et al., 1994; Kirby et al., 1999;
148 McCoy, 2001; Daniel and Pyle, 2006; Jones et al. 2010; Shah and Bell., 2012; Doe et al., 2013;
149 Mahan et al., 2013; Mako et al., 2015; Aronoff et al., 2016; Lytle, 2016, Bollen et al., 2022;
150 Daniel et al., 2022b), suggesting a convergent setting.

151

152 **The Grenville Orogeny**

153 The ~1.2–1.0 Ga Grenville orogeny along the SE margin of Laurentia resulted in the
154 emplacement of the ~1.1 Ga Pikes Peak Batholith in Colorado, but no significant deformation
155 (Whitmeyer and Karlstrom, 2007; Guitreau et al., 2016). Cambrian rifting in Colorado only
156 occurred in the Wet Mountains, and resulted in REE-rich alkaline intrusive rocks and veins
157 (Armbrustmacher, 1988). Elsewhere, Proterozoic deformation was overprinted by the Late
158 Cretaceous–Eocene Laramide orogeny (e.g., English et al., 2003; Kellogg et al., 2008) and
159 associated mineralization. Paleogene mineralization was concentrated within the Colorado
160 Mineral Belt (Fig. 2) and may or may not have been controlled by Proterozoic structures such as
161 shear zones (Tweto and Simms, 1963; Caine et al., 2010; Chapin, 2012). The latest deformation
162 was localized extension associated with the Oligocene and younger Rio Grande Rift, which

163 trends northward from Socorro, New Mexico to Leadville, Colorado (Olsen et al., 1987; Chapin
164 and Cather, 1994; Caine and Minor, 2009; Minor et al., 2013).

165

166 **GEOLOGY OF THE CENTRAL COLORADO FRONT RANGE**

167 Prominent Proterozoic structures of the central Colorado Front Range at the latitude of
168 Denver include at least three generations of folds and the Idaho Springs-Ralston shear zone
169 (IRSZ; Figs. 2, 3). The IRSZ is a NE-trending Proterozoic shear zone that was previously
170 interpreted to extend from the Mount Evans Batholith, ~10 km SE of Idaho Springs, CO, to the
171 eastern margin of the Front Range, ~10 km NNW of Golden, CO (e.g. Kellogg et al., 2008).
172 Madison Bzdok (née Lytle; Lytle, 2016) conducted detailed mapping along the shear zone and
173 concluded that it does not extend farther SW than Virginia Canyon Road, on the north side of
174 Idaho Springs (Figs. 2, 3). NE-trending shear zones of the central Colorado Front Range
175 including the IRSZ were initially interpreted as a suture zone that formed during ~1.8–1.6 Ga
176 accretion of small terranes and island arcs to the Proterozoic Wyoming Craton (Bowring and
177 Karlstrom, 1990; McCoy et al., 2005; Abbott and Cook, 2012). This interpretation was largely
178 based on the presence of tectonic *mélange* at the St. Louis Lake shear zone, ~40 km NNW of the
179 IRSZ (McCoy, 2001). The Proterozoic shear zones were reactivated between ~1.45 Ga and ~1.38
180 Ga (McCoy, 2001). These shear zones may or may not have controlled the location of Paleogene
181 mineralization that generally but not exclusively occurred along the Colorado Mineral Belt
182 (Tweto and Sims, 1963; McCoy, 2001). The interpretation of the IRSZ as a Paleoproterozoic
183 suture zone and its interpreted control on the location of the Colorado Mineral Belt has been
184 debated by Caine et al. (2010).

185 Based on detailed structural mapping, Lytle (2016; Fig. 3) demonstrated that the IRSZ is
186 not as extensive as previously interpreted. Additionally, a lack of pinch outs and offset of major
187 units, as well as similar deformation histories and metamorphic conditions on either side suggest
188 that the IRSZ did not form as a continental suture zone. Along the IRSZ, isoclinal F₁ folds are
189 overprinted by F₂ folds (Lytle, 2016; Figs. 3, 4). F₂ folds NW of the IRSZ have subvertical NE-
190 trending axial planes and plunge shallowly NE. SE of the IRSZ they also plunge shallowly NE,
191 but axial planes dip shallowly ENE. Lytle (2016) developed a model where isoclinal F₁ folds are
192 folded by asymmetric NW-side-up meter-scale F₂ folds, followed by a several km-scale NE-
193 plunging, NW-dipping F₃ folds (Fig. 4). NW-side-down movement along the IRSZ may have
194 been a result of flexural slip on the NW steeply dipping limb of the NE-plunging, NW-dipping
195 F₃ fold. U–Pb laser ablation inductively coupled mass spectrometry monazite dates revealed
196 ~1.68 Ga and ~1.43 Ga events, both within and adjacent to the IRSZ. Relationships between
197 microstructures and monazite grains suggest F₁ folds formed at ~1.68 Ga and F₂ and F₃ folding
198 and associated shearing along the IRSZ occurred at ~1.43 Ga. The relationship between shearing
199 and widespread folding at ~1.43 Ga suggests that Mesoproterozoic deformation, and the extent
200 of the Picuris orogeny, was much more extensive than solely reactivation along shear zones, as
201 previously interpreted (Shaw et al. 2001; McCoy et al., 2005).

202 Mapping and geochronology by Mahatma (2019), Powell (2020) and Shockley (2021) in
203 the Mount Evans and Montezuma areas SE of Idaho Springs indicated that folding in those areas
204 too was partly Paleoproterozoic and partly Mesoproterozoic. Therefore, pervasive folding as a
205 result of the Picuris orogeny affected a large part of the central Colorado front Range. In
206 addition, U–Pb detrital geochronology of a quartzite south of Mount Evans yielded a ~1.43 Ga
207 detrital zircon population (Fig. 5; Mahatma, 2019), indicating that some of the sedimentary rocks

208 were deposited during the Picuris orogeny. The ~1.43 Ga zircon population is interpreted as
209 detrital, and not metamorphic or hydrothermal, because grains show concentric and oscillatory
210 zoning. In addition, some ~1.43 Ga grains show zoned cores with unzoned metamorphic
211 overgrowths that were too narrow to date, but that suggest igneous zircon growth prior to
212 deposition and metamorphism of the quartzite. This is discussed in detail by Mahatma (2019).
213 The quartzite and other stratified rocks were metamorphosed shortly after deposition of the
214 quartzite as indicated by ~1.42 Ga and ~1.39–1.33 Ga metamorphic monazite in pelitic schist in
215 the area (Mahatma, 2019).

216

217 **GEOLOGY OF THE WET MOUNTAINS**

218 The Wet Mountains comprise a NW-trending fault-bounded block of primarily
219 Proterozoic rocks (Fig. 6). Metavolcanic and metasedimentary rocks are intruded by Paleo- and
220 Mesoproterozoic igneous rocks. Paleoproterozoic intrusive bodies include the foliated tonalite
221 and granodiorite of the ~1705 Ma Twin Mountain and Crampton Mountain plutons and the
222 weakly foliated to undeformed granodiorite of the ~1663 Ma Garell Peak pluton (Fig. 6;
223 Bickford et al., 1989). Mesoproterozoic intrusive rocks include the foliated 1442–1439 Ma Oak
224 Creek pluton (Figs. 6, 7), which ranges from quartz monzonite and monzogranite to leucogranite
225 (Bickford et al., 1989; Siddoway et al., 2000; Hernández-Montenegro et al., 2019); the unfoliated
226 1460 Ma West McCoy Gulch leucogranite pluton (Fig. 6; Cullers et al., 1993); and the 1371–
227 1362 Ma San Isabel pluton (Fig. 6), which is a monzogranite to syenogranite that is variably
228 deformed at exposed margins and generally undeformed within the main body of the pluton
229 (Cullers et al., 1992; Jones et al., 2010).

230 The southern part of the Wet Mountains contains extensive exposures of migmatite
231 gneiss (Figs. 6, 8). The central and southern Wet Mountains host intrusive bodies, including the
232 Oak Creek and San Isabel plutons, and an extensive network of sill and dike intrusions (Jones et
233 al., 2010; Levine et al., 2013). In the Greenhorn Mountain area south and west of the main body
234 of the San Isabel pluton, host rock-intrusion relationships are commonly unclear, because of the
235 extent of migmatization of host rock gneisses and because of the extensive network of
236 centimeter- to meter-scale felsic intrusions (Fig. 8; Jones et al., 2010; Levine et al., 2013). The
237 San Isabel pluton contains magmatic epidote (Cullers et al., 1992), suggesting mid-crustal
238 emplacement depths. Migmatite gneisses at the contact with the Oak Creek pluton record peak
239 metamorphic conditions of ~ 750 °C and ~ 7 kbar (Hernández-Montenegro et al., 2019).

240 Mesoproterozoic deformation, metamorphism, and igneous rock emplacement occurred
241 between ~ 1.43 Ga and 1.36 Ga and these processes were broadly coeval throughout the range
242 (Siddoway et al., 2000; Jones et al., 2010). In the northern Wet Mountains, Mesoproterozoic
243 deformation overprinted two generations of Paleoproterozoic fabrics, and strain was
244 concentrated in shear zones (Siddoway et al., 2000). In the southern Wet Mountains, researchers
245 interpret that extensive partial melt generation lead to the formation of melt networks that
246 accommodated lower crustal flow in response to regional compressive stresses (Jones et al.,
247 2010; Levine et al., 2013; Searle, 2013; Levine and Rahl, 2021).

248 The northern part of the Wet Mountains is well known for thorium and other rare earth
249 element (REE) mineralization associated with Cambrian-Ordovician alkaline intrusions,
250 including the McClure Mountain, Gem Park, and Democrat Creek complexes (Fig. 6). These
251 complexes are sequentially cross-cut by lamprophyre, syenite, and carbonatite dikes, and
252 mineralized quartz-barite-thorite veins (Armbrustmacher, 1988; Magnin et al., 2021). REE

253 mineralization occurs predominately within carbonatite dikes, quartz-barite-thorite veins, and
254 hydrothermally altered red syenite dikes (Armbrustmacher, 1988). Alkaline magmatic rocks in
255 the Wet Mountains may have been derived from a mantle melt, likely related to failed
256 intracontinental rifting during the Cambrian-Ordovician (Olson et al., 1977; Larson et al., 1985;
257 McMillan and McLemore, 2004; Magnin et al., 2021).

258

259 **FIELD TRIP DESCRIPTION AND STOPS**

260 We will first discuss how the Picuris orogeny reactivated or overprinted earlier structures,
261 and perhaps controlled the location of structures associated with Cambrian rifting, the
262 Cretaceous- Paleogene Laramide orogeny and subsequent Rio Grande Rift, and associated
263 mineralization. Stops 1–7 will give an overview of geology of the central Colorado Front Range,
264 including rocks and deformation associated with the Paleoproterozoic Yavapai/Mazatzal
265 orogenies and the Mesoproterozoic Picuris orogeny, and some of the Cretaceous- Paleogene
266 structures and mineralization associated with the Laramide orogeny. Stops 8 and 9 will also
267 focus on deformation and metamorphism associated with the Paleoproterozoic Yavapai/Mazatzal
268 orogenies and the Mesoproterozoic Picuris orogeny, and with Cambrian REE-bearing magmatic
269 rocks as a result of Cambrian rifting.

270

271 **DAY 1. CENTRAL COLORADO FRONT RANGE – INTRODUCTION TO THE** 272 **PROTEROZOIC YAVAPAI/MAZATZAL AND PICURIS OROGENIES**

273

274 **Leave conference center 7.00 am**

275 Drive 32 miles, 50 minutes (could make 10 minute restroom break along the way, at gas station
276 before field stop)

277

278 **Stop 1. Idaho Springs-Ralston shear zone 8.00-9.30 am; includes introduction talk**

279 Location: 39°47'11" N, 105°27'57" W; 2363m elevation

280 (coordinates at parking location; outcrops are across the road along the NW side to the NW and
281 the SE)

282

283 The outcrop shows a variety of schist and gneiss with subvertical NE-trending foliation
284 and steep lineation (Fig. 9). The shear sense is predominantly NW-side-down and locally NW-
285 side up. One biotite-muscovite schist yielded ~1.67 Ga, ~1.63 Ga and ~1.48 Ga in-situ U-Pb LA-
286 ICPMS monazite ages, and another yielded ~1.62 Ga and ~1.44 Ga ages (Lytle, 2016). The ages
287 are consistent with other ages of deformation along the Idaho Springs-Ralston shear zone, and of
288 folds away from the shear zone (Lytle, 2016).

289 **Questions for discussion:** What are the shear direction and shear sense? Was this shear zone a
290 suture zone or a smaller scale shear zone? How is it related to folding in the area? How would
291 one find out?

292

293 Drive 5 miles, 8 minutes (could make 10 minute restroom break along the way, at gas station
294 before field stop; same as before)

295

296 **Stop 2. Mesoproterozoic pegmatite along top-to-the-south shear 9.45-10.15 am**

297 Location: 39°44'47" N, 105°23'51" W; 2108m elevation

298 (coordinates at outcrop; park ~50 m to the north along the east side of the road in the pull-out
299 and walk south)

300

301 Southeast of the Idaho Springs-Ralston shear zone there are tens of meter-scale shear structures
302 displaying top-to-the-south ductile-brittle shear along shallowly-north-dipping shear planes.

303 These may be the latest structures associated with the Picuris orogeny, after folding, or they may
304 represent late flexural slip on the SE limb of a NW-dipping anticline during folding associated
305 with the Picuris orogeny. The pegmatite along the shear plane at this stop (Fig. 10A-D) yielded a
306 weighted average of $^{207}\text{Pb}/^{206}\text{Pb}$ LA-ICPMS ages of 1441 ± 83 (N=4, MSWD = 2.3), with
307 inheritance of primarily 1771 ± 24 Ma grains (N=9, MSWD = 0.55) and as old as 1913 ± 67 Ma
308 (Fig. 10E).

309

310 **Questions for discussion:** What is the significance of these shears? Are they related to folding in
311 the area, and to the Idaho Springs-Ralston shear zone on the other 'limb' of the large-scale NW-
312 dipping NE-plunging synform? How would one find out?

313

314 **Drive 8.5 miles, 15 minutes (restroom on site at the Edgar Mine)**

315

316 **Stop 3. Edgar Experimental Mine 10.30 am-12.30 pm**

317 Location: $39^{\circ}44'50''$ N, $105^{\circ}31'31''$ W; 2399m elevation

318 (coordinates at outcrop; park ~50 m to the north along the east side of the road in the pull-out
319 and walk south)

320

321 The Edgar mine, the Colorado School of Mines Experimental Mine (Fig. 11), stems from
322 the “Rush to the Rockies” mining period. In the 1870s, it produced high-grade silver, gold, lead
323 and copper. It is now part of the Colorado School of Mines and an educational laboratory for
324 those learning to find, develop, and process natural resources. In addition to educating Colorado
325 School of Mines’ Mining Engineering students, it provides educational tours for the public and
326 school groups.

327 The oldest rocks are Paleoproterozoic gneiss and schist (Fig. 11C) that are along-strike
328 with and arguably part of the Idaho Springs-Ralston shear zone. However, the mylonite zone that
329 is characteristic of the Idaho Springs-Ralston shear zone ends less than 700 m to the NE, where
330 the last outcrops can be seen on the Virginia Canyon ‘Oh-My-God’ (for its twists and turns,
331 which are now much less scary than in the past) Road. In Idaho Springs, a zone of NE-trending
332 foliation exists associated with folding at upper amphibolite facies, but no mylonite zone. This
333 led to the conclusion that the Idaho Springs-Ralston shear zone is not a suture zone, but an effect
334 of regional folding (Lytle, 2019; Fig. 4).

335 Cretaceous-Paleogene quartz veins and mineralization in the mine (Fig. 11D) are close to
336 parallel in and around the Edgar Mine, but on careful inspection they can be seen to crosscut at
337 very low angle.

338

339 ***Question for discussion:*** Is Cretaceous- Paleogene mineralization, magmatism, faulting and
340 veining controlled by Proterozoic structures?

341

342 **Lunch 12.30-1.00 pm (can make this shorter probably)**

343 Pizza at BeauJo’s in Idaho Springs.

344

345 ***Question for discussion:*** What is better: thin-crust pizza or Colorado style mountain pie?

346

347 **Drive 2.5 miles, 7 minutes**

348

349 **Stop 4. Mega sigma-clast and other shear structures 1.15-1.30 pm**

350 Location: 39°44'39" N, 105°29'16" W; 2281m elevation

351

352 Look east on the cliff across the road to find a mega sigma-clast (Fig. 12A) and other large-scale
353 shear structures (Fig. 12B). The shear sense is top to the south, as in stop 2. Structures like this
354 exist throughout this area SE of the Idaho Springs-Ralston shear zone (and elsewhere?) and give
355 something to look at when stuck in ski traffic.

356

357 ***Question for discussion:*** Continue discussion of stop 2. Also, what causes such large-scale
358 structures to form? Is it because of rheology contrast, or because of brittle shear localization, or
359 something else? Where else have you seen such large-scale shear structures?

360

361 **Drive 7 miles, 12 minutes**

362

363 **Stop 5. Sheared Mount Evans batholith 1.45-2.30 pm (probably include)**

364 Location: 39°41'38" N, 105°37'02" W; 2689m elevation

365

366 This outcrop looks like steeply WNW-dipping sheared rock with NW-side-up movement (Fig.
367 13) and may have been interpreted as the Idaho Springs-Ralston Shear Zone in the past.
368 However, it is too northerly-trending for that, and foliations and shear zones within ~500m to the
369 SW, S and SE, and on a separate outcrop ~4 km to the SW along West Chicago Creek Road have
370 various orientations. Shear zones are only local here and their significance is not clear and
371 probably minor.

372

373 **Questions for discussion:** Why is the Idaho Springs-Ralston Shear Zone here? Does it reactivate
374 earlier NE-trending structures? How does it relate to other NE-trending shear zones of Colorado,
375 some of which are interpreted as suture zones?

376

377 **Stop 6. Weakly foliated Mount Evans batholith 2.40-3.10 pm**

378 Location: 39°42'13" N, 105°36'29" W; 2612m elevation

379

380 Here, the Mount Evans batholith looks much less deformed than the previous outcrop (Fig. 14A),
381 and has a weak foliation that is more typical for the Mount Evans batholith. The batholith was
382 initially interpreted as having primarily flow foliations (Aleinikoff et al., 1993), but Powell
383 (2020) noted that most foliations dip moderately NW (Fig. 14B) and are probably tectonic. This
384 may imply the latest shortening direction of the Picuris orogeny was NW, while the top-to-the-
385 south ductile brittle structures of stops 3 and 4 imply that it was south-directed. Interestingly,
386 other ~1.4 Ga plutons and other deformed rocks also show evidence for NW-directed shortening
387 in Colorado (Gonzales et al., 1996; Jones et al., 2010; Shah and Bell, 2012), New Mexico
388 (Grambling and Coddling, 1982) and Arizona (Doe and Daniel, 2019), while in the Picuris

389 mountains of New Mexico (Daniel et al., 2013) and the Montezuma mining district of Colorado
390 (Shockley, 2021) it is north-directed.

391

392 **Questions for discussion:** What was the latest shortening direction of the Picuris orogeny? What
393 might it have been earlier? How does it fit with shortening in New Mexico and Arizona and with
394 shear zone reactivation?

395

396 **Stop 7. Folded migmatitic biotite gneiss 3.20-3.50 pm**

397 Location: 39°42'50" N, 105°34'48" W; 2483m elevation

398

399 Migmatitic biotite gneiss is isoclinally folded, and subsequently refolded by moderately NE-
400 plunging open to close (NW-side-up?) F₂ folds (Fig. 15). The lineation is steep and pre-or syn-
401 F₂ folding. This location is along strike with the Idaho Springs-Ralston Shear Zone of stop 1, but
402 here it has died out.

403

404 **Questions for discussion:** Why does the Idaho Springs-Ralston Shear Zone die out toward the
405 SW? Is it related to folding (flexural flow)?

406

407 **Drive 150 miles, 2.5-3.0 hours**

408 **Stay overnight in Walsenburg, CO**

409

410 **DAY 2. WET MOUNTAINS – PROTEROZOIC DEFORMATION AND**

411 **METAMORPHISM AND CAMBRIAN RIFTING**

412 Drive from Best Western Rambler in Walsenburg, depart 7:15am

413 Drive ~38 miles, 55-75 min

414

415 **Stop 8. Garnet biotite migmatite gneiss**

416 Parking Location: 37°53'30.73"N, 105° 6'23.85"W; 2670m elevation

417 Walk ~0.9 miles (heading up in elevation) along the Cisneros Trail

418

419 This section of the Cisneros Trail contains semi-continuous outcrop exposure of biotite
420 migmatite gneiss, garnet biotite migmatite gneiss, and amphibolite (Fig. 9). We will walk the
421 first mile of the trail. The Cisneros Trail is a ~10-mile path from this stop location to the San
422 Isabel recreation area. The trail continues past this field trip stop through exposures of granitic
423 sill and dike intrusions. The northern section of the trail passes through the main body of the San
424 Isabel pluton, but exposure is poor. Stop 8 will highlight migmatite textures and mineralogy (Fig.
425 9). These migmatite outcrops are characteristic of the southern Wet Mountains, where host rock-
426 intrusion relationships are cryptic or obscured.

427

428 ***Questions for discussion:*** What can we interpret from migmatite textures in outcrop about the
429 structural or temporal relationship between partial melt formation and felsic intrusions in the
430 southern Wet Mountains? What might different structural interpretations imply about tectonic
431 models of southwestern North America in the Proterozoic?

432

433 Drive from Cisneros trailhead to downtown Westcliffe, CO

434 Drive 48 miles, ~1 hour, 15 min

435

436 Stop for lunch in Westcliffe

437

438 Drive from Westcliffe along Oak Creek Grade (County Road 143) to East Bear Trailhead pull-
439 out

440 Drive 20 miles, ~40 minutes

441

442 Stop 9. Oak Creek pluton

443 Parking location: 38° 18' 19.764" N, 105° 15' 16.83" W; 2255m elevation

444

445 We will examine a section of the Oak Creek pluton exposed along the road (Fig. 8). The Oak
446 Creek is a foliated Mesoproterozoic pluton with a crystallization age of 1442–1439 Ma (Bickford
447 et al., 1989; Cullers et al., 1993; Jones et al., 2010). Its fabrics are generally concordant with host
448 rock fabrics (Siddoway et al., 2000; Jones et al., 2010). Adjacent host rocks include felsic gneiss,
449 amphibolite, and migmatite gneiss (Siddoway et al., 2000; Jones et al., 2010; Levine et al., 2013;
450 Hernández-Montenegro et al., 2019). The Oak Creek ranges in composition from quartz-
451 monzonite to monzogranite to leucogranite (Bickford et al., 1989; Cullers et al., 1993) and is also
452 ferroan in composition (Cullers et al., 1993; Frost et al., 2001; Hernández -Montenegro et al.,
453 2019).

454

455 *Questions for discussion:* How can we reconcile the structural evidence of syntectonic
456 emplacement of this Mesoproterozoic pluton with the ferroan geochemical character of the
457 pluton?

458

459 **DISCUSSION**

460 We conclude this field guide with some thoughts for discussion. Previously,
461 Mesoproterozoic orogenic and other Earth processes have been interpreted as different from
462 those in the Paleoproterozoic, and Neoproterozoic/Phanerozoic (e.g., Bradley et al., 2011; Brown
463 et al., 2020; Spencer et al., 2021; Liu et al., 2022). Here, we give a summary of some of the
464 observations and interpretations. Bradley et al. (2011) compiled various datasets and
465 demonstrated various minima, including the number of passive margins, detrital zircons,
466 greenstone-belt collisions, eclogites, granulites, carbonatites, and orogenic gold. Perhaps the
467 quiescence explains the “Boring Billion” of Holland (2006), which was based on a period of
468 little variation in atmospheric oxygen levels. Brown et al. (2020) observed that T/P ratios of
469 metamorphic rocks were higher in the Mesoproterozoic than at any other time in the Earth’s
470 history. High T/P conditions were accompanied by high $^{176}\text{Hf}/^{177}\text{Hf}$ ratios and low $\delta^{18}\text{O}$ values in
471 zircon, indicating more juvenile crust in the Mesoproterozoic (Brown et al., 2020). A high
472 volume of massif-type anorthosites also indicate high T/P conditions and zircon Eu/Eu^* ratios
473 indicate thin crust (Spencer et al., 2021). Low T/P ratios in metamorphic rocks are characteristic
474 for plate boundaries, (Liu et al., 2022), suggesting that there were fewer plate boundaries in the
475 Mesoproterozoic than before and after that time. Low T/P rocks are especially characteristic for
476 blueschist and eclogite facies rocks and and associated with subduction. While present in the
477 Paleoproterozoic, these became especially abundant in the Neoproterozoic when there was a
478 transition to modern plate tectonic processes (Brown et al., 2020; Liu et al., 2022).

479 Paleogeographic reconstructions show that Paleoproterozoic supercontinent may never
480 have broken up fully and transitioned into Rodinia towards the end of the Mesoproterozoic

481 without too much plate movement (e.g. Pisarevsky et al., 2014, Martin et al. 2020). Along the SE
482 margin of Laurentia, there may have been subduction during most of the Mesoproterozoic, and
483 perhaps slab rollback, associated juvenile crust formation, and possible accretion of juvenile
484 crust (cf. Brown et al., 2020; Liu et al., 2022; Daniel et al., 2022a). Plate tectonic processes may
485 have slowed down during this period, or alternatively, the Mesoproterozoic may have been
486 characterized by hot, thin, and low orogens (Spencer et al., 2021).

487 These observations and interpretations may explain why the Picuris orogeny is so
488 difficult to recognize and was largely overlooked until the past decade. It is still difficult to
489 envision what the entire orogenic belt might have looked like, including locations of the arc,
490 fore-arc and back-arc, and other components of the orogenic belt. We will discuss these issues
491 during the trip, and hope we will have inspiring discussion about the intricacies of the
492 Mesoproterozoic.

493

494 **ACKNOWLEDGMENTS**

495 We thank current and past Colorado School of Mines graduate students Ben Magnin,
496 Asha Mahatma, Logan Powell and Dustin Shockley for discussion and/or contribution. We much
497 benefited from discussion with Jonathan Caine, Mike Doe and John Ridley. Chris Holm-Denoma
498 and Zhaoshan Chang carried out U-Pb LA-ICPMS geochronology.

499

500 **REFERENCES CITED**

501 Abbott, L., and Cook, E., 2012, Geology Underfoot along Colorado's Front Range: Montana,
502 Mountain Press Publishing Company, 93 p.

503 Aleinikoff, J.N., Reed, J.C., and DeWitt, E.H., 1993, The Mount Evans batholith in the Colorado
504 Front Range: Revision of its age and reinterpretation of its structure: Geological Society
505 of America Bulletin, v. 105, p. 791–806, [https://doi.org/10.1130/0016-](https://doi.org/10.1130/0016-7606(1993)105<0791:TMEBIT>2.3.CO;2)
506 [7606\(1993\)105<0791:TMEBIT>2.3.CO;2](https://doi.org/10.1130/0016-7606(1993)105<0791:TMEBIT>2.3.CO;2).

507 Allen, J.L., and Shaw, C.L., 2011, Seisomogenic structure of a crystalline thrust fault: fabric
508 anisotropy and coeval pseudotachylyte-mylonitic pseudotachylyte in the Grizzly Creek
509 Shear Zone, Colorado, in Fagereng, A°, Toy, V. G. & Rowland, J. V., eds., Geology of
510 the Earthquake Source: A Volume in Honour of Rick Sibson: Geological Society,
511 London, Special Publications, v. 359, p. 135–151.

512 Anderson, J.L., and Morrison, J., 2005, Ilmenite, magnetite, and peraluminous Mesoproterozoic
513 anorogenic granites of Laurentia and Baltica: Lithos, v. 80, p. 45–60,
514 <https://doi.org/10.1016/j.lithos.2004.05.008>.

515 Armbrustmacher, T.J., 1988, Geology and resources of thorium and associated elements in the
516 Wet Mountains area, Fremont and Custer counties, Colorado: United States Geological
517 Survey Profession Paper 1049, 10.3133/pp1049F

518 Aronoff, R.F., Andronicos, C.L., Vervoort, J.D., and Hunter, R.A., 2016, Redefining the
519 metamorphic history of the oldest rocks in the southern Rocky Mountains: Geological
520 Society of America Bulletin, v. 128, p. 1207–1227, <https://doi.org/10.1130/B31455.1>.

521 Bennett, V.C., and DePaolo, D.J., 1987, Proterozoic crustal history of the western United States
522 as determined by neodymium isotopic mapping: Geologic Society of America Bulletin, v.
523 99, p. 674–685, doi: 10.1130/0016-7606(1987)99<674:PCHOTW>2.0.CO;2.

524 Bickford, M.E., Shuster, R.D., and Boardman, S.J., 1989, U-Pb geochronology of the
525 Proterozoic volcano-plutonic terrane in the Gunnison and Salida area, Colorado, in

526 Grambling, J.A., and Tewksbury, B.J., eds., Proterozoic geology of the southern Rocky
527 Mountains: Geological Society of America Special Paper 235, p. 33–48.

528 Bollen, E.M., Stowell, H.H., Aronoff, R.F., Stotter, S.V., Daniel, C.G., McFarlane, C.R.M.,
529 Vervoort, J.D., 2022, Reconciling garnet Lu-Hf and Sm-Nd and monazite U-Pb ages for a
530 prolonged metamorphic event, northern New Mexico: *Journal of Petrology*, v. 63,
531 doi.org/10.1093/petrology/egac031

532 Bowring, S.A., and Karlstrom, K.E., 1990, Growth, stabilization, and reactivation of Proterozoic
533 lithosphere in the southwestern United States: *Geology*, v. 18, p. 1203–1206,
534 doi:10.1130/0091-7613(1990)018<1203:GSAROP>2.3.CO;2.

535 Bradley D.C., 2008, Passive margins through Earth history: *Earth-Science Review*, v. 91, p. 1-
536 26.

537 Brown, M., Johnson, T., Gardiner, N.J., 2020, Plate tectonics and the Archean Earth: *Annual*
538 *Review of Earth and Planetary Sciences*, v. 48, p. 291-320.

539 Bryant, Bruce, Miller, R.D., and Scott, G.R., 1973, Geologic map of the Indian Hills quadrangle,
540 Jefferson County, Colorado: U.S. Geological Survey, scale 1:24,000.

541 Caine, J.S., and Minor S.A., 2009. Structural and geochemical characteristics of faulted
542 sediments and inferences on the role of water in deformation, Rio Grande Rift, New
543 Mexico. *Geological Society of America Bulletin* 121, 1325–1340.

544 Caine, J.S., Ridley, J., and Wessel, Z.R., 2010, To reactivate or not to reactivate – nature and
545 varied behavior of structural inheritance in the Proterozoic basement of the eastern
546 Colorado Mineral Belt over 1.7 billion years of earth history: *Geological Society of*
547 *America Field Guide*, v. 18, p. 119-140, doi: 10.1130/2010.0018(06).

548 Chapin, C.E., 2012, Origin of the Colorado Mineral Belt: *Geosphere*, v. 8, p. 28—43,
549 doi:10.1130/GES00694.1.

550 Chapin, C.E., and Cather, S.M., 1994, Tectonic setting of the axial basins of the northern and
551 central Rio Grande rift, in Keller, G.R., and Cather, S.M., eds., *Basins of the Rio Grande*
552 *Rift: Structure, stratigraphy, and tectonic setting: Geological Society of America Special*
553 *Paper 291*, p. 5—25, doi:10.1130/SPE291-p5.

554 Condie, K.C., 1986, Geochemistry and tectonic setting of Early Proterozoic supracrustal rocks in
555 the southwestern United States: *Journal of Geology*, v. 94, p. 845–864.

556 Cullers, R.L., Griffin, T., Bickford, M.E., and Anderson, J.L., 1992, Origin and chemical
557 evolution of the 1360 Ma San Isabel Batholith, Wet Mountains, Colorado: A mid-crustal
558 granite of anorogenic affinities: *Geological Society of America Bulletin*, v. 104, p. 316–
559 328, doi: 10.1130/0016-7606(1992)104<0316:OACEOT>2.3.CO;2.

560 Cullers, R. L., Stone, J., Anderson, J. L., Sassarini, B., and Bickford, M. E., 1993, Petrogenesis
561 of Mesoproterozoic Oak Creek and West McCoy Gulch plutons, Colorado: An example
562 of cumulate unmixing of a mid-crustal, two mica granite of anorogenic affinity:
563 *Precambrian Research*, v. 62, p. 139–169.

564 Daniel, C.G., Pfeifer, L.S., Jones, J.V. III, and McFarlane, C.M., 2013, Detrital zircon evidence
565 for non-Laurentian provenance, Mesoproterozoic (ca. 1490-1450 Ma) deposition and
566 orogenesis in a reconstructed orogenic belt, northern New Mexico, USA: Defining the
567 Picuris orogeny: *Geological Society of America Bulletin*, v. 125, n. 9-10, p. 1423-1441.

568 Daniel, C.G., Aronoff, R., Indares, A.D., and Jones, J.V. III, 2022a, Laurentia in transition
569 during the Mesoproterozoic: observations and speculation on the ca. 1500-1340 Ma
570 tectonic evolution of the south Laurentian margin, in Whitmeyer, S.J., Williams, M.L.,

571 Kellett, D.A., and Tikoff, B., eds., *Laurentia: Turning Points in the Evolution of a*
572 *Continent: Geological Society of America Memoir 220,*
573 [https://doi.org/10.1130/2022.1220\(08\)](https://doi.org/10.1130/2022.1220(08))

574 Daniel, C.G., Indares, A., Medaris, L.G., Jr., Aronoff, R., Malone, D., and Schwartz, J., 2022b,
575 *Linking the Pinware, Baraboo, and Picuris orogenies: Recognition of a trans-Laurentian*
576 *ca. 1520–1350 Ma orogenic belt, in Whitmeyer, S.J., Williams, M.L., Kellett, D.A., and*
577 *Tikoff, B., eds., Laurentia: Turning Points in the Evolution of a Continent: Geological*
578 *Society of America Memoir 220, [https://doi.org/10.1130/2022.1220\(11\)](https://doi.org/10.1130/2022.1220(11)).*

579 Daniel, C.G., and Pyle, J.M., 2006, *Monazite-Xenotime thermochronometry and Al₂SiO₅*
580 *reaction textures in the Picuris Range, northern New Mexico, USA: new evidence for a*
581 *1450-1400 Ma orogenic event: Journal of Petrology, v. 47, n. 1, p. 97–118.*

582 Doe, M.F., and Daniel, G.G., 2019, *Evidence for Mesoproterozoic ca. 1470-1444 Ma regional*
583 *deformation of the Mazatzal Group and equivalent rocks in the type area of the Mazatzal*
584 *orogeny, Tonto Basin, Arizona, in Pearthree, P.A., ed., Geologic excursions in*
585 *southwestern North America: Geological Society of America Field Guide 55, p. 1–36,*
586 [doi.org/10.1130/2019.0055\(10\)](https://doi.org/10.1130/2019.0055(10)).

587 Doe, M.F., Jones, J.V. III, Karlstrom, K.E., Thrane, K., Frei, D., Gehrels, G., Pecha, M., 2012,
588 *Basin formation near the end of the 1.60-1.45 Ga tectonic gap in southern Laurentia:*
589 *Mesoproterozoic Hess Canyon Group of Arizona and implications for ca. 1.5 Ga super-*
590 *continent configurations: Lithosphere, v. 4, n. 1, p. 77-88.*

591 Doe, M.F., Jones, J.V. III, Karlstrom, K.E, Dixon, B., Gehrels, G.E., 2013, *Using detrital zircon*
592 *ages and Hf isotopes to identify ca. 1.48-1.45 Ga sedimentary basins and fingerprint*

593 potential sources of exotic 1.6-1.5 Ga grains in southwestern Laurentia: Precambrian
594 Research, v. 231, p. 409-421. <http://dx.doi.org/10.1016/j.precamres.2013.03.002>.

595 du Bray, E.A., Holm-Denoma, C.S., Lund, K., and Premo, W.R., 2018, Review of the
596 Geochemistry and Metallogeny of Approximately 1.4 Ga Granitoid Intrusions of the
597 Conterminous United States: U.S. Geological Survey Scientific Investigations Report
598 2017-5111, 34 p., <https://doi.org/10.3133/sir20175111>.

599 English, J. M., Johnston, S. T., and Wang, K., 2003, Thermal modelling of the Laramide
600 orogeny: Testing the flat-slab subduction hypothesis: Earth and Planetary Science
601 Letters, v. 214, p. 619–632.,

602 Frost, B.R., Barnes, C.G., Collins, W.J., Arculus, R.J., Ellis, D.J., Frost, C.D., 2001, A
603 geochemical classification for granitic rocks: Journal of Petrology, v. 42, p. 2033–2048.

604 Frost, C.D., and Frost, B.R., 2022, Petrologic constraints on the origin of Proterozoic ferroan
605 granites of the Laurentian margin, in Whitmeyer, S.J., Williams, M.L., Kellett, D.A., and
606 Tikoff, B., eds., Laurentia: Turning Points in the Evolution of a Continent: Geological
607 Society of America Memoir 220, [https://doi.org/10.1130/2022.1220\(10\)](https://doi.org/10.1130/2022.1220(10)).

608 Gable, 2000, Geologic map of the Proterozoic rocks of the central Front Range, Colorado: U.S.
609 Geological Survey, IMAP 2605, scale 1:100,000.

610 Gonzales, D.A., Karlstrom, K.E., and Siek, G., 1996, Syncontractional crustal anatexis and
611 deformation during emplacement of the 1435 Ma Electra Lake gabbro, Needle
612 Mountains, Colorado: The Journal of Geology, v. 104, p. 215–223, doi: 10.1086
613 /629815.

614 Goodge, J.W., and Vervoort, J.D., 2006, Origin of Mesoproterozoic A-type granites in Laurentia:
615 Hf isotope evidence: *Earth and Planetary Science Letters*, v. 243, p. 711–731,
616 <https://doi.org/10.1016/j.epsl.2006.01.040>.

617 Gower, C.F., and Krogh, T.E., 2002, A U-Pb geochronological review of the Proterozoic history
618 of the eastern Grenville Province: *Canadian Journal of Earth Sciences*, v. 39, p. 795–829,
619 <https://doi.org/10.1139/e01-090>.

620 Groulier, P.-A., Indares, A.D., Dunning, G., Mouhksil, A., 2020, Andean style 1.50–1.35 Ga arc
621 dynamics in the southeastern Laurentian margin: the rifting and reassembly of Quebecia:
622 *Terra Nova*, p. 1-8, doi:10.1111/ter.12482.

623 Guitreau, M., Mukasa, S.B., Blichert-Tift, J., and Fahnestock, M.F., 2016, Pikes Peak batholith
624 (Colorado, USA) revisited: A SIMS and LA-ICP-MS study of zircon U–Pb ages
625 combined with solution Hf isotopic compositions: *Precambrian Research*, v. 280, p. 179–
626 194.

627 Hernández-Montenegro, D., Andronicos, C.L., Zuluaga, C.A., and Aronoff, R.A., 2019, Effects
628 of melt loss, melt retention, and protolith composition on differentiation of anatectic
629 metapelites: A case study of the Wet Mountains, Colorado: *Lithos*, v. 344–345, p. 425–
630 439, <https://doi.org/10.1016/j.lithos.2019.06.032>.

631 Holland, H. D., 2006, The oxygenation of the atmosphere and oceans, *Philosophical*
632 *Transactions of the Royal Society B: Biological Sciences*, v. 361(1470), p. 903–915.
633 <https://doi.org/10.1098/rstb.2006.1838>

634 Holland, M.E., Grambling, T.A., Karlstrom, K.E., Jones III, J.V, Nagotko, K.N., Daniel, C.G.,
635 2020, Geochronologic and Hf-isotope framework of Proterozoic rocks from central New

636 Mexico, USA: Formation of the Mazatzal crustal province in an extended continental
637 margin arc: *Precambrian Research*, v. 347, doi:10.1016/j.precamres.2020.105820.

638 Jessup, M.J., Jones, J.V., Karlstrom, K.E., Williams, M.L., Connelly, J.N., and Heizler, M.T.,
639 2006, Three Proterozoic orogenic episodes and an intervening exhumation event in the
640 Black Canyon of the Gunnison region, Colorado: *The Journal of Geology*, v. 114, p. 555-
641 576, doi:10.1086/506160.

642 Jones, J.V., III, and Connelly, J.N., 2006, Proterozoic tectonic evolution of the Sangre de Cristo
643 Mountains, southern Colorado, U.S.A.: *Rocky Mountain Geology*, v. 41, p. 79–116, doi:
644 10.2113/gsrocky.41.2.79.

645 Jones, J.V., III, Connelly, J.N., Karlstrom, K.E., Williams, M.L., and Doe, M.F., 2009, Age,
646 provenance, and tectonic setting of Paleoproterozoic quartzite successions in the
647 southwestern United States: *Geological Society of America Bulletin*, v. 121, p. 247–264.

648 Jones, J.V., III, Siddoway, C.S., and Connelly, J.N., 2010, Characteristics and implications of ca.
649 1.4 Ga deformation across a Proterozoic mid-crustal section, Wet Mountains, Colorado,
650 USA: *Lithosphere*, v. 2, p. 119–135, <https://doi.org/10.1130/L78.1>.

651 Jones, J.V., III, Daniel, C.G., Frei, D., and Thrane, K., 2011, Revised regional correlations and
652 tectonic implications of Paleoproterozoic and Mesoproterozoic metasedimentary rocks in
653 northern New Mexico, USA: New findings from detrital zircon studies of the Hondo
654 Group, Vadito Group, and Marqueñas Formation: *Geosphere*, v. 7, no. 4, p. 974–991,
655 <https://doi.org/10.1130/GES00614.1>.

656 Karlstrom, K.E., and Bowring, S.A., 1988, Early Proterozoic assembly of tectonostratigraphic
657 terranes in southwestern North America: *The Journal of Geology*, v. 96, p. 561–576.

658 Karlstrom, K.E., and Humphreys, G., 1998, Influence of Proterozoic accretionary boundaries in
659 the tectonic evolution of western North America: Interaction of cratonic grain and mantle
660 modification events: *Rocky Mountain Geology*, v. 33, p. 161–179.

661 Kellog, K.S., Shroba, R.R., Bryant, B., and Premo, W.R., 2008, Geologic map of the Denver
662 west 30' x 60' quadrangle, north-central Colorado: U.S. Geological Survey, scale
663 1:100,000.

664 Kirby, E., Karlstrom, K.E., Andronicos, C.L., and Dallmeyer, R.D., 1995, Tectonic setting of the
665 Sandia pluton: An orogenic 1.4 Ga granite in New Mexico: *Tectonics*, v. 14, p. 185–201,
666 <https://doi.org/10.1029/94TC02699>.

667 Kopera, J., 2003, Monazite Geochronology of the Ortega Quartzite: Documenting the Extent of
668 1.4 Ga Tectonism in Northern New Mexico and across the Orogen [M.S. thesis]:
669 Amherst, University of Massachusetts, 130 p.

670 Larson, E.E., Patterson, P.E., Curtis, G., Drake, K., Mutschler, F.E., 1985, Petrologic,
671 paleomagnetic, and structural evidence of a Paleozoic rift system in Oklahoma, New
672 Mexico, Colorado, and Utah: *Geological Society of America Bulletin*, v. 96, n. 11, p.
673 1364-1372.

674 Levine, J.S.F. and Rahl, J.M., 2021, Subgrain Boundaries as Sites of Melt Generation and
675 Pathways for Melt Flow: Implications for Rheology From Combined Chemical and
676 Quantitative Orientation Analysis: *Journal of Geophysical Research: Solid Earth*, v. 126,
677 no. 6, p. e2020JB020487.

678 Levine, J.S., Mosher, S., Siddoway, C.S., 2013, Relationship between syndeformational partial
679 melting and crustal-scale magmatism and tectonism across the Wet Mountains, central
680 Colorado: *Lithosphere* v. 5, p. 456–476.

681 Liu, Y., Mitchell, R.N., Brown, M., Johnson, T.E., and Pisarevsky, S., 2022, Linking
682 metamorphism and plate boundaries over the past 2 billion years: *Geology*,
683 <https://doi.org/10.1130/G49637.1>

684 Lytle, M., 2016, The Proterozoic history of the Idaho Springs-Ralston shear zone: Evidence for
685 widespread ca. 1.4 Ga orogenic event in Central Colorado [M.Sc. thesis]: Golden,
686 Colorado School of Mines, 89 p.

687 Magnin, B., Kuiper, Y.D., Barkmann, P.E., 2021. Preliminary structural analysis of alkaline
688 dikes and mineralized veins in the Wet Mountains, south-central Colorado: connecting
689 rare earth element mineralization to Cambrian rifting. *GSA Abstracts with Programs*. Vol
690 53, No. 6., doi: 10.1130/abs/2021AM-367101

691 Mahan, K.H., Allaz, J.A., Baird, G.B., and Kelly, N.M., 2013, Proterozoic metamorphism and
692 deformation in the northern Colorado Front Range, *in* Abbott, L.D., and Hancock, G.S.,
693 eds., *Classic Concepts and New Directions: Exploring 125 Years of GSA Discoveries in*
694 *the Rocky Mountain Region: Geological Society of America Field Guide*, v. 33, p. 185-
695 204, doi:10.1130/2013.0033(06).

696 Mahatma, A., 2019, The Proterozoic history of the southern half of the Mount Evans 7.5 minute
697 quadrangle: evidence for ca. 1.4 Ga orogenic event in the central Front Range, Colorado:
698 MS Thesis, Colorado School of Mines, Golden CO, 88 p.

699 Mako, C.A., Williams, M.L., Karlstrom, K.E., Doe, M.F., Powicki, D., Holland, M.E., Gehrels,
700 G., and Pecha, M., 2015, Polyphase Proterozoic deformation in the Four Peaks area,
701 central Arizona, and relevance for the Mazatzal orogeny: *Geosphere*, v. 11, no. 6, p.
702 1975–1995, doi:10.1130/GES01196.1.

703 Martin, E. L., Spencer, C. J., Collins, W. J., Thomas, R. J., Macey, P. H., & Roberts, N. M. W.,
704 2020, The core of Rodinia formed by the juxtaposition of opposed retreating and
705 advancing accretionary orogens: *Earth-Science Reviews*, v. 211, 103413.
706 <https://doi.org/10.1016/j.earscirev.2020.103413>

707 McCoy, A.M., 2001, The Proterozoic ancestry of the Colorado Mineral Belt: ca. 1.4 Ga shear
708 zone system in central Colorado [M.Sc. thesis]: Albuquerque, University of New Mexico,
709 160 p.

710 McCoy, A.M., Karlstrom, K.E., Shaw, C.A., and Williams, M.L., 2005, The Proterozoic ancestry
711 of the Colorado Mineral Belt: 1.4 Ga shear zone system in central Colorado, in
712 Karlstrom, K.E., and Keller, G.R., eds., *The Rocky Mountain Region: An Evolving
713 Lithosphere: American Geophysical Union Geophysical Monograph 154*, p. 71–90,
714 <https://doi.org/10.1029/154GM06>.

715 McMillan, N.J., and McLemore, V.T., 2004, Cambrian–Ordovician magmatism and extension in
716 New Mexico and Colorado: *New Mexico Bureau of Geology & Mineral Resources
717 Bulletin 160*, p. 1-11.

718 Medaris, L.G. Jr., Singer, B.S., Jicha, B.R., Malone, D.H., Schwartz, J.J., Stewart, E.K., Van
719 Lankvelt, A., Williams, M.L., and Reiners, P.W., 2021, Early Mesoproterozoic evolution
720 of midcontinental Laurentia: Defining the geon 14 Baraboo orogeny: *Geoscience
721 Frontiers*, v. 12, Article 101174, doi:10.1016/j.gsf.2021.101174.

722 Minor, S.A., Hudson, M.R., Caine, J.S., Thompson, R.A., 2013, Oblique transfer of --
723 extensional strain between basins of the middle Rio Grande rift, New Mexico: fault
724 kinematic and paleostress constraints: *Geological Society of America Special Paper 494*,
725 345–382.

726 Nyman, M.W., Karlstrom, K.E., Kirby, E., and Graubard, C.M., 1994, Mesoproterozoic
727 contractional orogeny in western North America: Evidence from ca. 1.4 Ga plutons:
728 *Geology*, v. 22, p. 901–904, [https://doi.org/10.1130/0091-](https://doi.org/10.1130/0091-7613(1994)022<0901:MCOIWN>2.3.CO;2)
729 [7613\(1994\)022<0901:MCOIWN>2.3.CO;2](https://doi.org/10.1130/0091-7613(1994)022<0901:MCOIWN>2.3.CO;2).

730 Olsen, K.H., Baldrige, W.S., Callender, J.F., 1987, Rio Grande rift: an overview:
731 *Tectonophysics*, v. 143, p. 119–139.

732 Olson, J.C., Marvin, R.F., Parker, R.L., and Mehnert, H.H., 1977, Age and tectonic setting of
733 lower Paleozoic alkalic and mafic rocks, carbonatites, and thorium veins in south-central
734 Colorado: *U.S. Geological Survey Journal of Research*, v. 5, p. 673—687

735 Pedrick, J.N., Karlstrom, K.E., and Bowring, S.A., 1998, Reconciliation of conflicting tectonic
736 models for Proterozoic rocks in northern New Mexico: *Journal of Metamorphic Geology*,
737 v. 16, p. 687–707, doi:10.1111/j.1525-1314.1998.00165.x.

738 Pisarevsky, S.A., Elming, S.Å., Pesonen, L.J., and Li, Z.X., 2014, Mesoproterozoic
739 paleogeography: Supercontinent and beyond: *Precambrian Research*, v. 244, p. 207–225,
740 <https://doi.org/10.1016/j.precamres.2013.05.014>.

741 Powell, L., 2020. The Proterozoic geology of the northern half of the Mount Evans 7.5-minute
742 quadrangle. M.S. Thesis, Colorado School of Mines, Golden, CO, USA, 58 pp.

743 Searle, M., 2013, Crustal melting, ductile flow, and deformation in mountain belts: Cause and
744 effect relationships: *Lithosphere*, v. 5, no. 6, p. 547-554.

745 Selverstone, J., Hodgins, M., Aleinikoff, J.N., and Fanning, C.M., 2000, Mesoproterozoic
746 reactivation of a Paleoproterozoic transcurrent boundary in the northern Colorado Front
747 Range: Implications for ~1.7- and 1.4-Ga tectonism: *Rocky Mountain Geology*, v. 35, p.
748 139–162, doi: 10.2113/35.2.139.

749 Shah, A.A., and Bell, T.H., 2012, Ninety million years of orogenesis, 250 million years of
750 quiescence and further orogenesis with no change in PT: Significance for the role of
751 deformation in porphyroblast growth: *Journal of Earth System Science*, v. 121, no. 6, p.
752 1365-1399.

753 Shaw, C.A., Karlstrom, K.E., Williams, M.L., Jercinovic, M.J., and McCoy, A.M., 2001,
754 Electron microprobe monazite dating of ca. 1.71–1.65 Ga and ca. 1.45–1.38 Ga
755 deformation in the Homestake shear zone, Colorado: Origin and early evolution of a
756 persistent intracontinental tectonic zone: *Geology*, v. 29, no. 8, p. 739–742, doi:
757 10.1130/0091-7613(2001)029<0739:EMMDOC>2.0.CO;2.

758 Shaw, C.A., Allen, J.L., 2007, Field rheology and structural evolution of the Homestake shear
759 zone, Colorado: *Rocky Mountain Geology*, v. 42, n. 1, p. 31-56.

760 Sheridan, D.M., and Marsh, S.P., 1976, Geologic map of the Squaw Pass quadrangle, Clear
761 Creek, Jefferson, and Gilpin Counties, Colorado: U.S. Geological Survey, scale 1:24,000.

762 Sheridan, D.M., Reed, J.C., Jr., and Bryant, Bruce, 1972, Geologic map of the Evergreen
763 quadrangle, Jefferson County, Colorado: U.S. Geological Survey, 1:24,000.

764 Shockley, D., 2021. Proterozoic structural history of the Montezuma mining district in the
765 central Colorado Front Range. M.S. Thesis, Colorado School of Mines, Golden, CO,
766 USA, 101 pp.

767 Siddoway, C.S., Givot, R.M., Bodle, C.D., and Heizler, M.T., 2000, Dynamic versus anorogenic
768 setting for Mesoproterozoic plutonism in the Wet Mountains, Colorado: Does the
769 interpretation depend on level of exposure?: *Rocky Mountain Geology*, v. 35, p. 91-111.

770 Sims, P.K., 1964, Geologic Map of the Central City Quadrangle, Colorado: U.S. Geological
771 Survey, scale 1:24,000.

772 Sims, P.K., and Gable, D.J., 1964, Geology of Precambrian rocks, Central City district,
773 Colorado: Geological Survey Professional Paper 474-C: Washington, United States
774 Government Printing Office, p. C1-C51.

775 Spencer, C.J., Mitchell, R.N., Brown, M., 2021, Enigmatic Mid-Proterozoic orogens: hot, thin,
776 and low: Geophysical Research Letters, v. 48, e2021GL093312.

777 Taylor, 1976, Geologic map of the Black Hawk quadrangle, Gilpin, Jefferson, and Clear Creek
778 Counties, Colorado: U.S. Geological Survey, scale 1: 24,000.

779 Tucker, R.D., and Gower, C.F., 1994, A U-Pb geochronological framework for the Pinware
780 terrane, Grenville Province, southeast Labrador: The Journal of Geology, v. 102, p. 67–
781 78, <https://doi.org/10.1086/629648>.

782 Tweto, O., and Sims, P.K., 1963, Precambrian Ancestry of the Colorado Mineral Belt:
783 Geological Society of America Bulletin, v. 74, p. 991-1014.

784 Wells, J.D., 1967, Geology of the Eldorado Springs quadrangle, Boulder and Jefferson Counties,
785 Colorado: U.S. Geological Survey Bulletin 1221-D, p. D1-D85, scale 1: 24,000.

786 Whitmeyer, S.J., and Karlstrom, K.E., 2007, Tectonic model for the Proterozoic growth of North
787 America: Geosphere, v. 3, p. 220–259.

788 Widmann, B.L., Kirkham, R.M., and Beach, S.T., 2000, Geologic map of the Idaho Springs
789 quadrangle, Clear Creek County, Colorado: Colorado Geological Survey, scale 1: 24,000.

790 Windley, B.F., 1993, Proterozoic anorogenic magmatism and its orogenic connection: Geological
791 Society [London] Journal, v. 150, p. 39–50.

792 Wooden, J.L., and DeWitt, E., 1991, Pb isotope evidence for a major Early Proterozoic crustal
793 boundary in western Arizona, *in* Karlstrom, K.E., ed., Proterozoic geology and ore deposits
794 of Arizona: Arizona Geological Society Digest, v. 19, p. 27–50.

795 Wooden, J.L., Stacey, J.S., Doe, B., Howard, K.A., and Miller, D.M., 1988, Pb isotopic evidence
796 for the formation of Proterozoic crust in the southwestern United States, *in* Ernst, W.G.,
797 ed., *Metamorphism and crustal evolution of the western United States: Rubey Volume VII*:
798 Englewood Cliffs, New Jersey, Prentice Hall, p. 68–86.

799 Wrucke, C.T., and Wilson, R.F., 1967, Geologic map of the Boulder quadrangle, Boulder County,
800 Colorado: U.S. Geological Survey, scale 1:24,000.

801 Young, E.J., 1991, Geologic map of the East Portal quadrangle, Boulder, Gilpin, and Grand
802 Counties, Colorado: U.S. Geological Survey, scale 1: 24,000.

803

804 **Figure Captions**

805 Figure 1. Simplified geologic map of Proterozoic age provinces for North America and
806 Proterozoic rocks exposed in the western U.S., (modified from Holland et al., 2020; Daniel et al.,
807 2022a). Dashed black lines indicate the approximate area of the Pinware–Baraboo–Picuris (PBP)
808 Orogen. Abbreviations: Pic–Picuris Mountains; SR–Salt River Canyon.

809
810 Figure 2. Simplified map of the southwestern United States showing Proterozoic crustal blocks.
811 Modified after Jones et al. (2010; cf. Condie, 1986; Bennett and DePaolo, 1987; Karlstrom and
812 Bowring, 1988; Wooden et al., 1988; Wooden and DeWitt, 1991). Colorado Mineral Belt
813 indicated with dashed line. After Mahatma (2019).

814
815 Figure 3. Geologic map of the Idaho Springs-Ralston shear zone (IRSZ) area from Lytle (2016),
816 after Gable (2000; cf. Sims, 1964; Sims and Gable, 1964; Wells, 1967; Wrucke and Wilson,
817 1967; Sheridan et al., 1972; Bryant et al., 1973; Sheridan and Marsh, 1976; Taylor, 1976; and
818 Young, 1991). Automated Mineralogy (AM) samples and map areas as described in detail by
819 Lytle (2016) indicated.

820
821 Figure 4. Cross section sketch showing proposed deformation and timing of deformation from
822 Lytle (2016). (A) Regional metamorphism at ~ 1.68 Ga (D1). (B) Picuris orogeny at ~ 1.45 - 1.40
823 Ga (D2). (C) Picuris orogeny at ~ 1.45 - 1.40 Ga (D3).

824
825 Figure 5. U-Pb LA-ICPMS zircon data from a quartzite (sample 366; Fig. 2). (A) Error ellipses
826 are 2σ and data that are $>10\%$ discordant gray. (B) Relative probability diagram showing

827 concordant data. (C) Float bar chart with weighted averages of $^{207}\text{Pb}/^{206}\text{Pb}$ ages for concordant
828 data. (D, E) Field photographs of quartzite looking NE.

829

830 Fig. 6. Geologic map of the Wet Mountains after Jones et al. (2010).

831

832 Fig. 7. Outcrop photo of the foliated Oak Creek pluton (left) and a photo of stop location 9
833 (right), with roadside exposure of the Oak Creek pluton.

834

835 Fig. 8. Outcrop photos showing typical textures of migmatites in the southern Wet Mountains,
836 including quartz-feldspar migmatite, biotite migmatite, and garnet-biotite migmatite. Note
837 isoclinal, ptygmatic, and refolded folds, shear bands, and anatectic garnet.

838

839 Figure 9. Idaho Springs-Ralston shear zone outcrop images.

840

841 Figure 10. (A-D) outcrop pictures, showing pegmatite along top-to-the-south shear. C is from
842 Google Earth. (E) U-Pb LA-ICPMS zircon data (error ellipses are 2σ), with weighted averages of
843 $^{207}\text{Pb}/^{206}\text{Pb}$ ages indicated.

844

845 Figure 11. The Edgar Mine, the Colorado School of Mines Experimental Mine. (A) Geology
846 graduate students in front of the entrance. (B) The USGS underground classroom. (C) NW-side-
847 up fold. (D) Pyrite vein. (E) location map of the Edgar Mine (red lines). Quartz-plagioclase
848 gneiss and quartz-plagioclase-biotite gneiss in blue and quartz-biotite-hornblende gneiss and
849 biotite-microcline-pegmatite in brown.

850

851 Figure 12. Mega-shear structures indicating top-to-the-south movement.

852

853 Fig. 13. (A) Outcrop photo. (B) west-side-up S-C fabric.

854

855 Fig. 14. (A) Outcrop photo, looking SW. (B) Poles to foliation in the Mount Evans batholith at Mount

856 Evans (from Powell, 2020).

857

858 Fig. 15. (A) F_1 folds in migmatitic biotite gneiss looking down to the NE along an F_2 fold hinge. (B) F_1

859 folds in migmatitic biotite gneiss looking down to the NW.

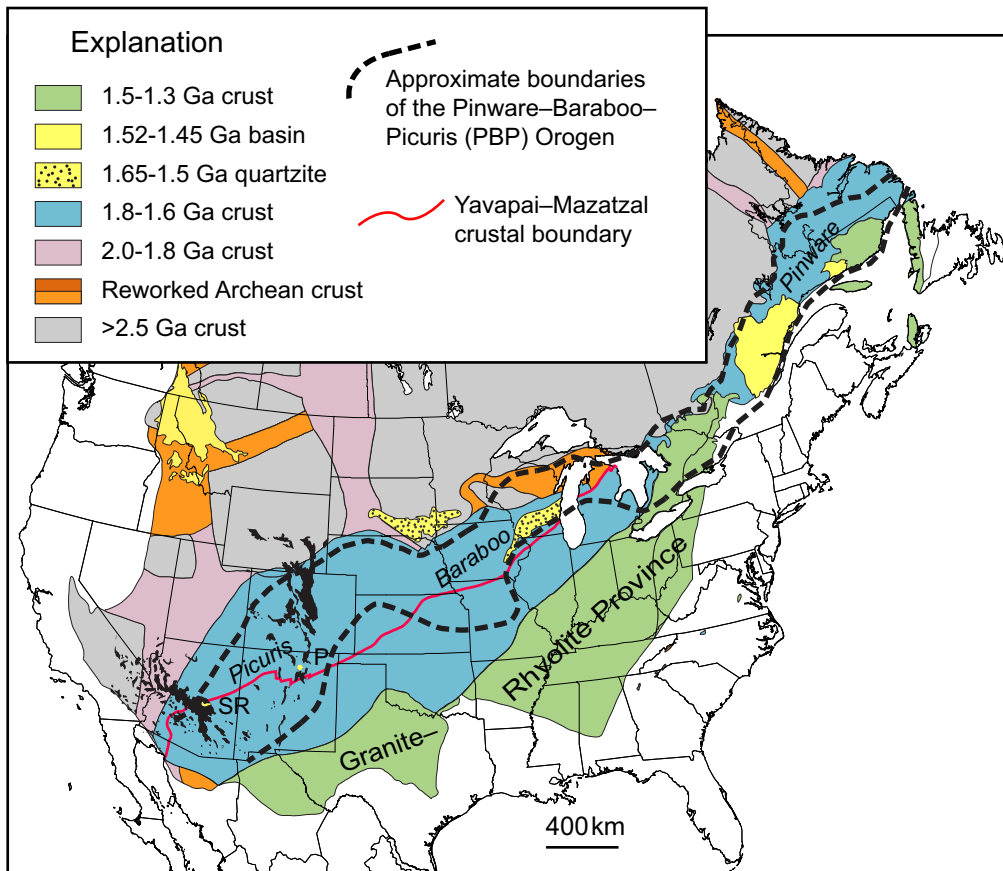


Figure 1

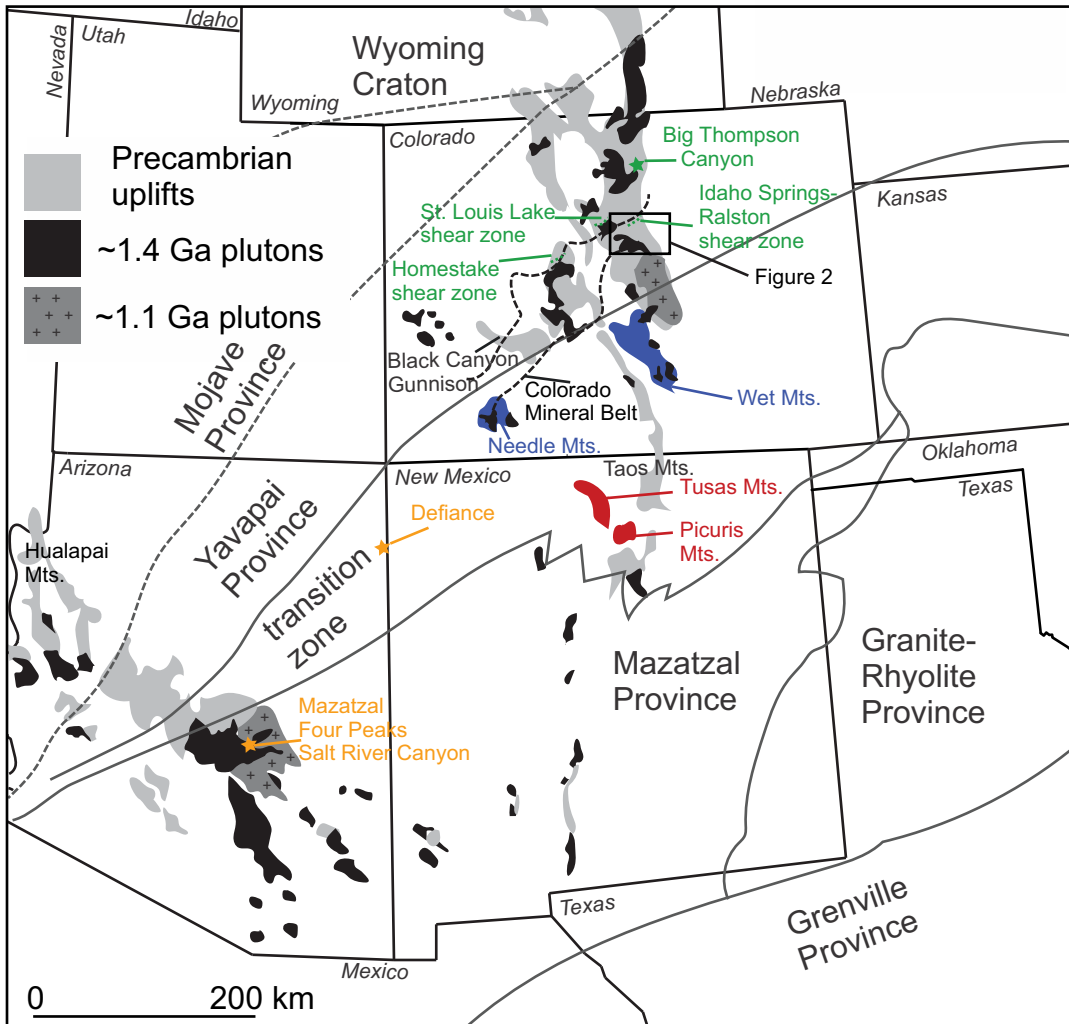


Figure 2

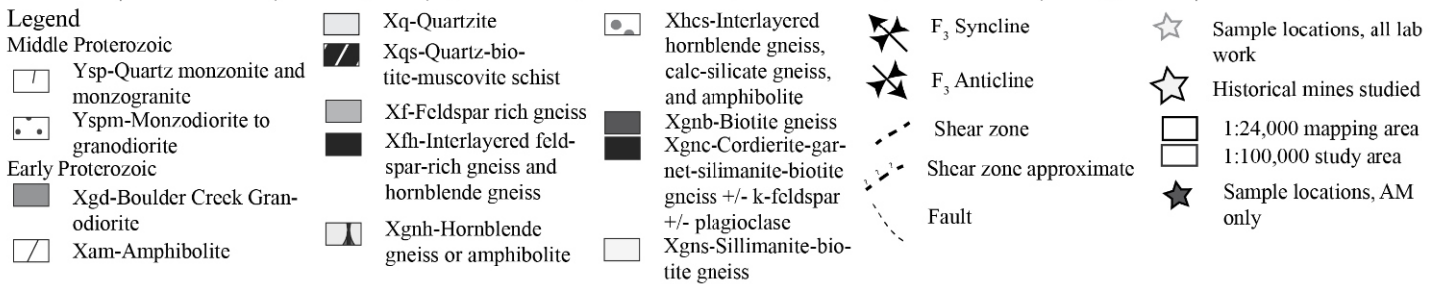
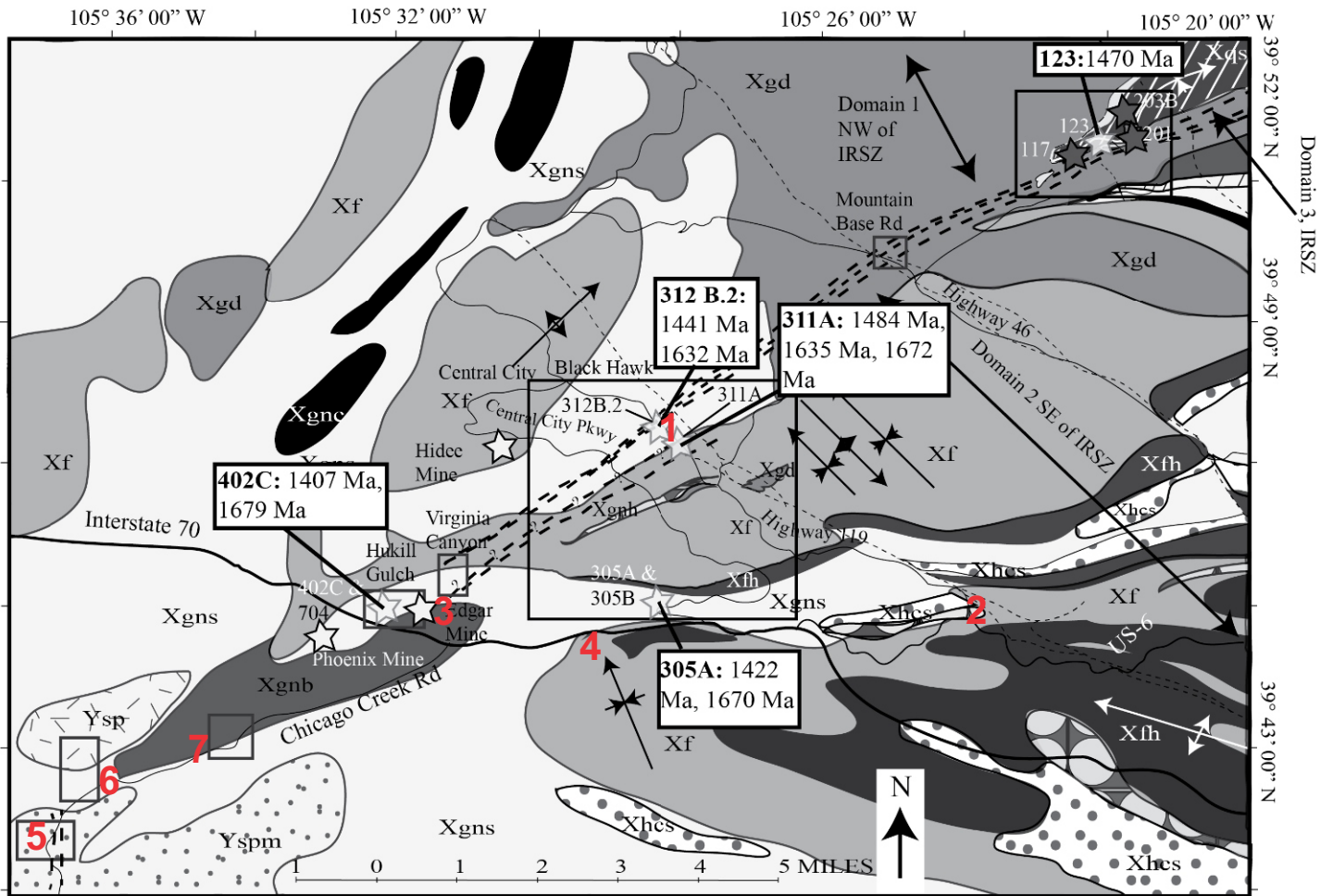


Figure 3

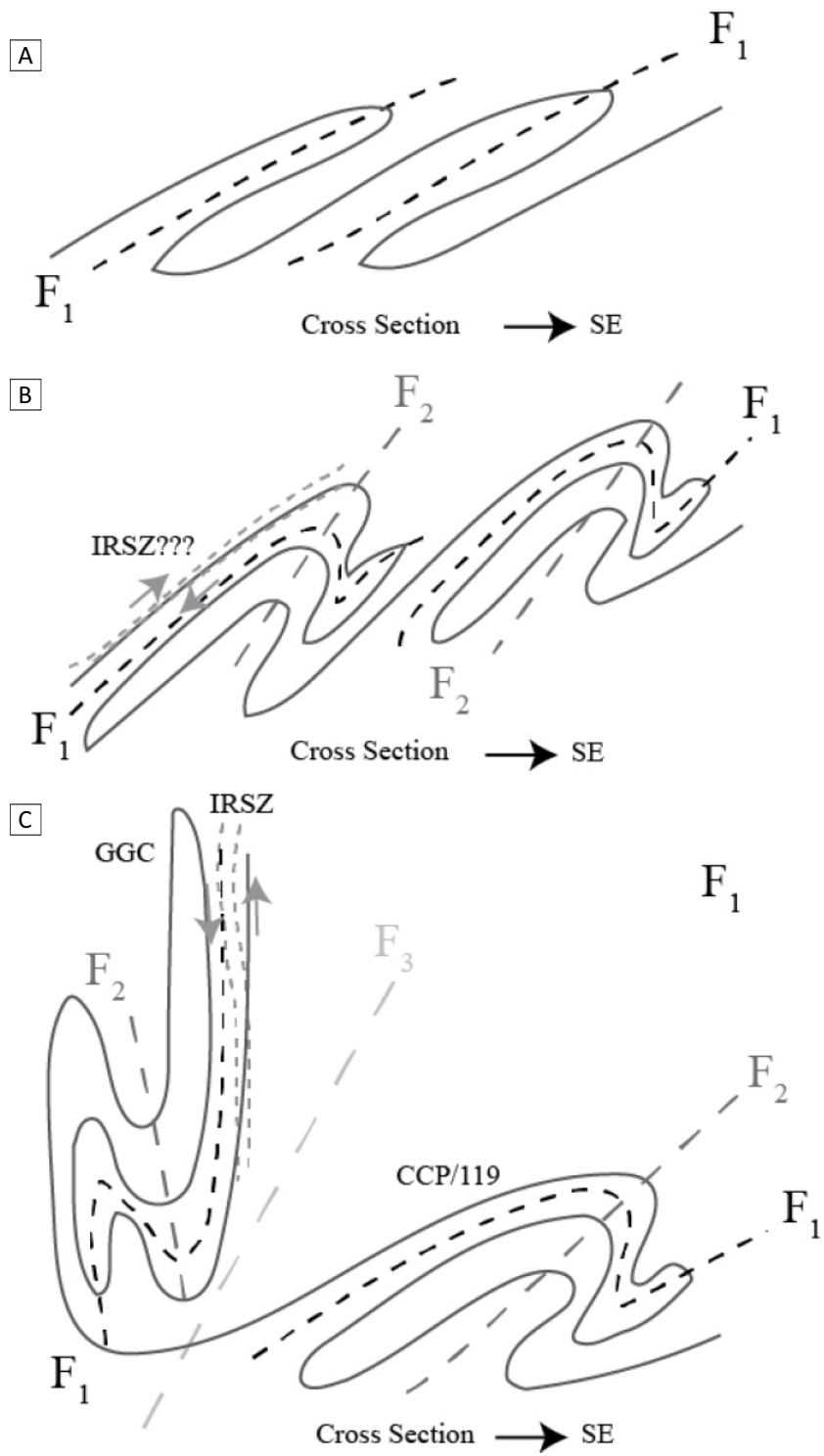


Figure 4

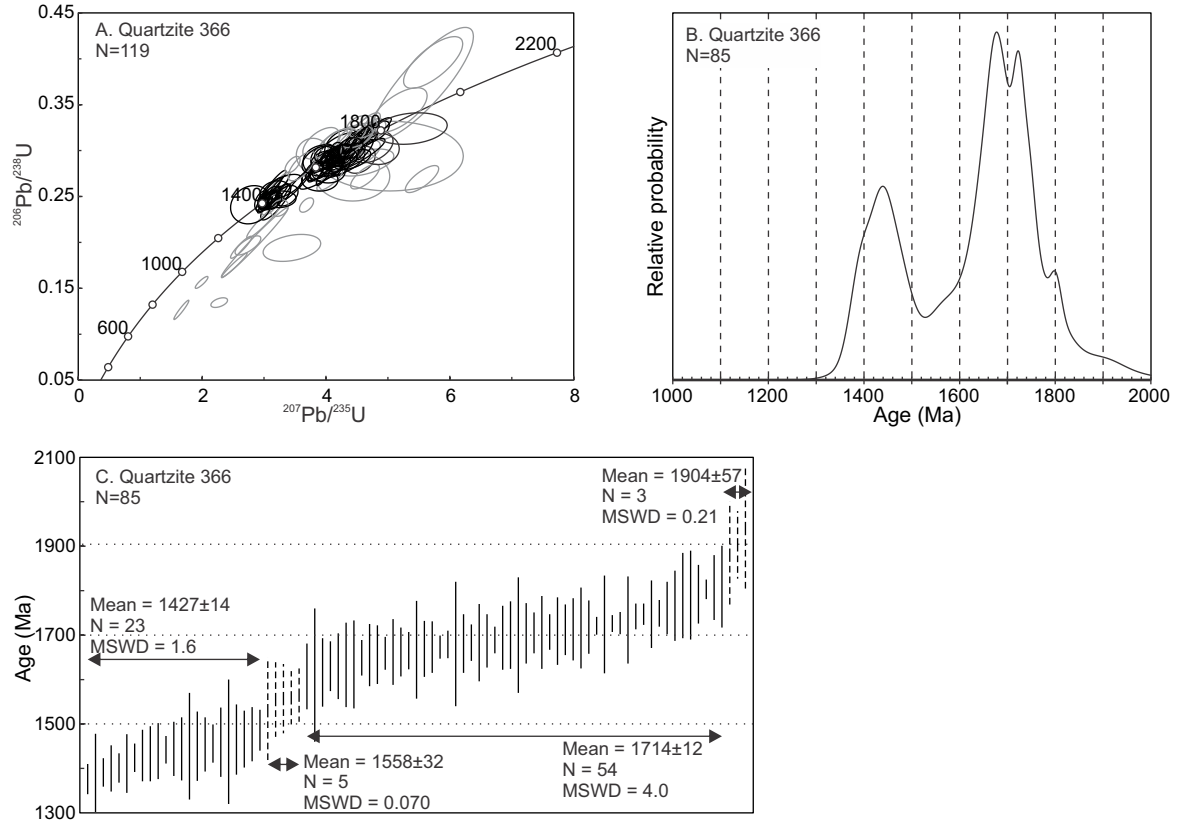


Figure 5

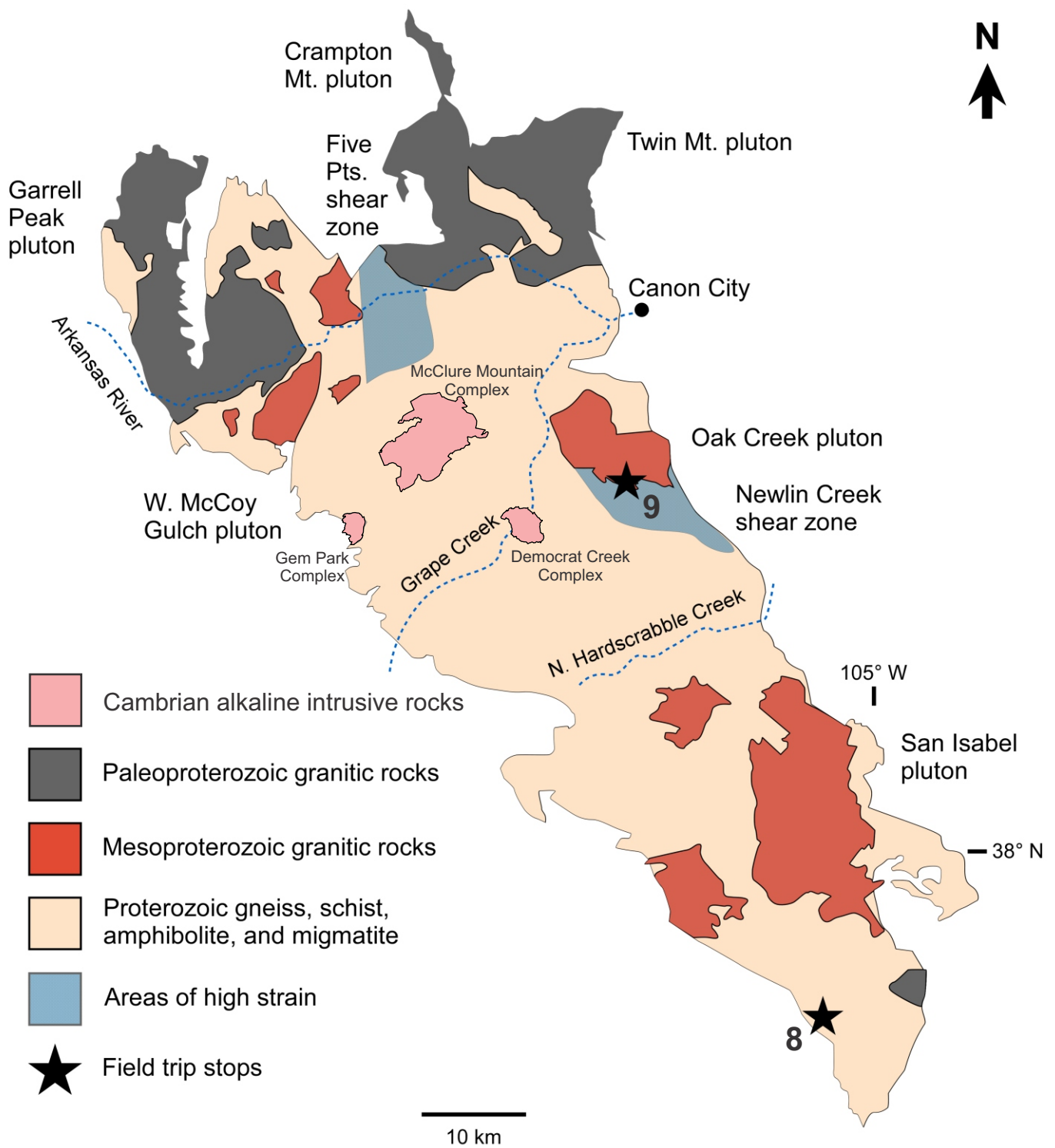


Figure 6



Figure 7



Figure 8



Figure 9

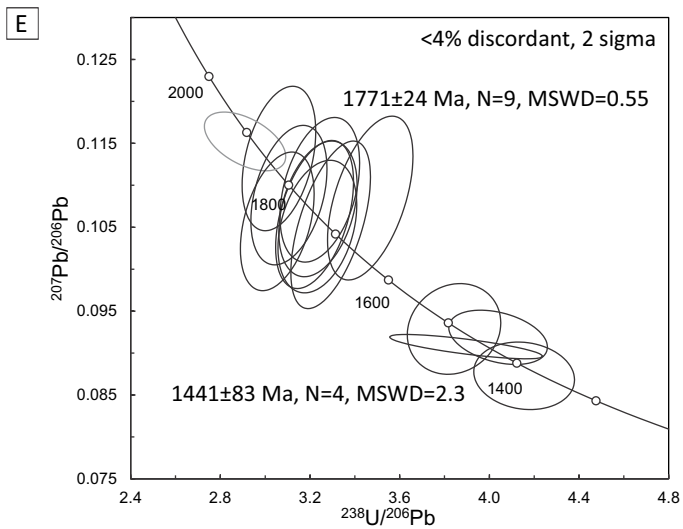
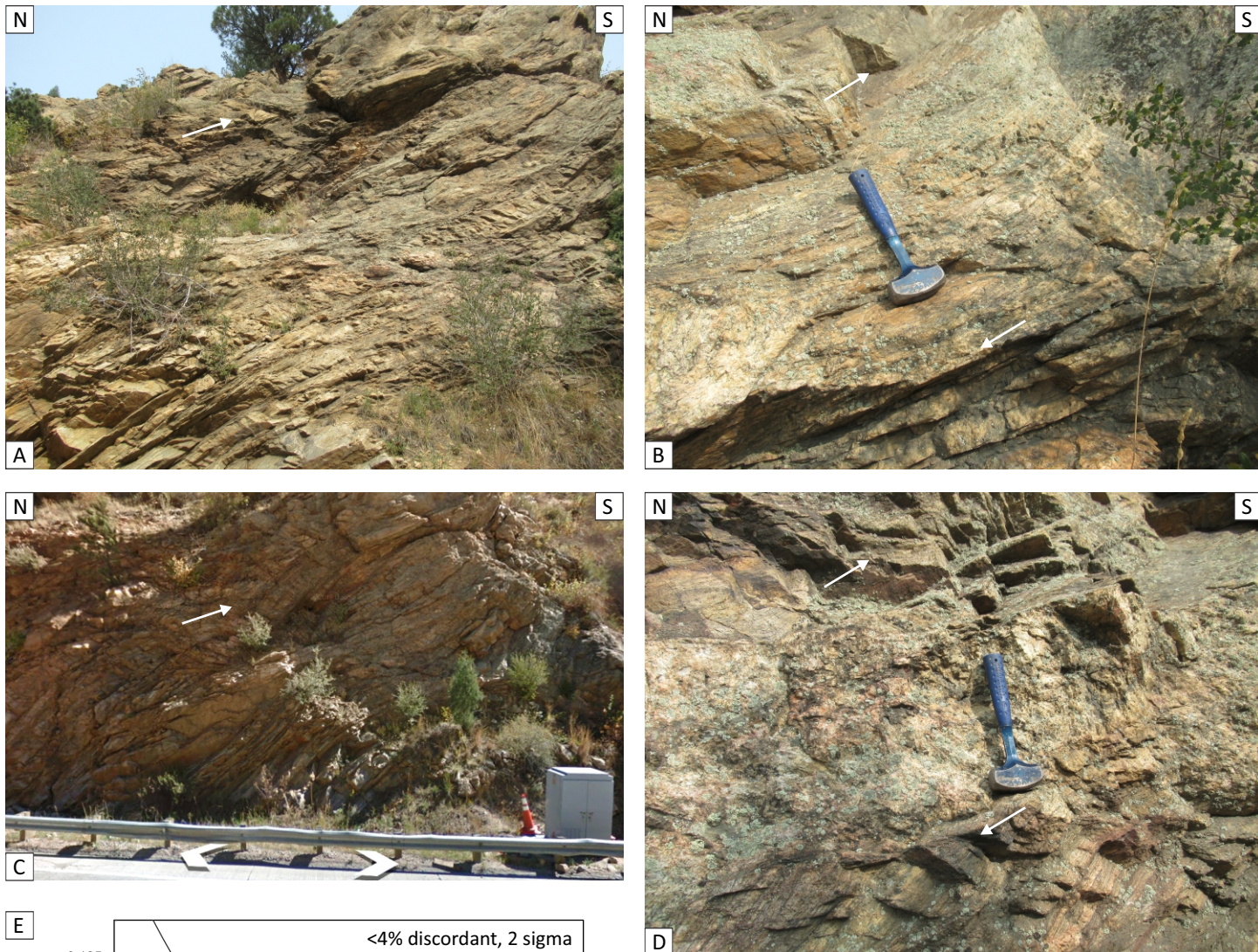


Figure 10

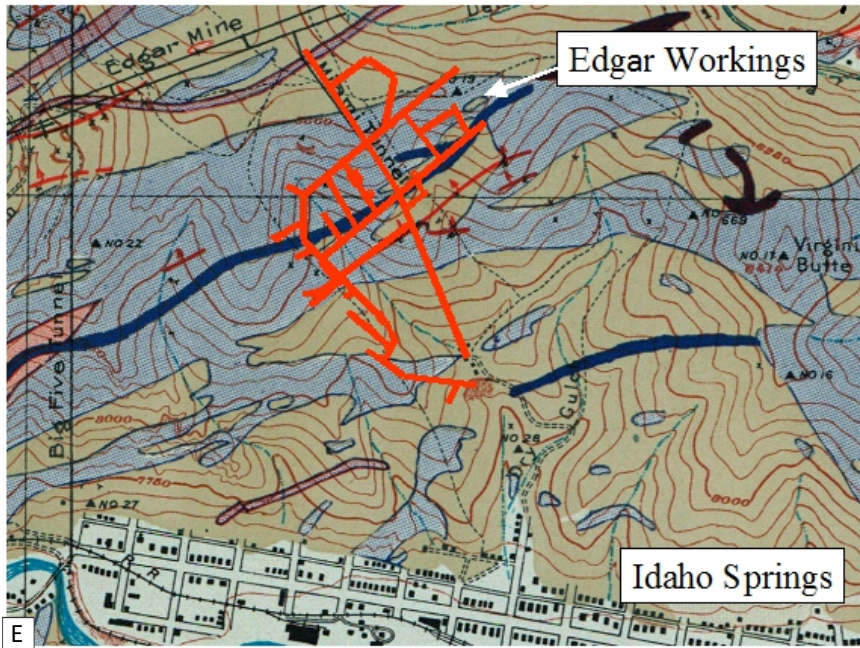


Figure 11



Figure 12



Figure 13

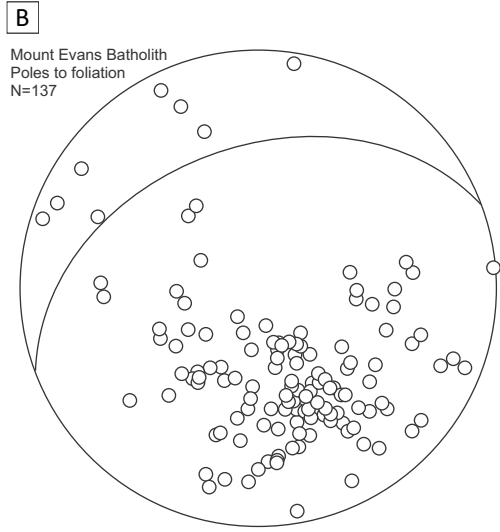


Figure 14

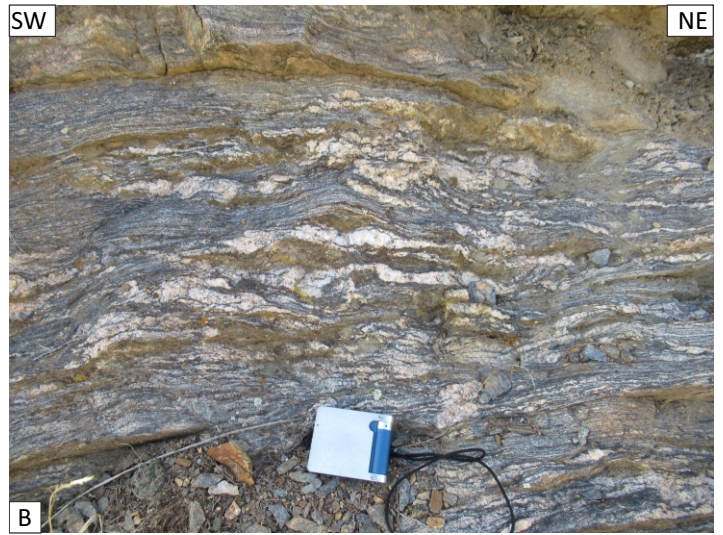
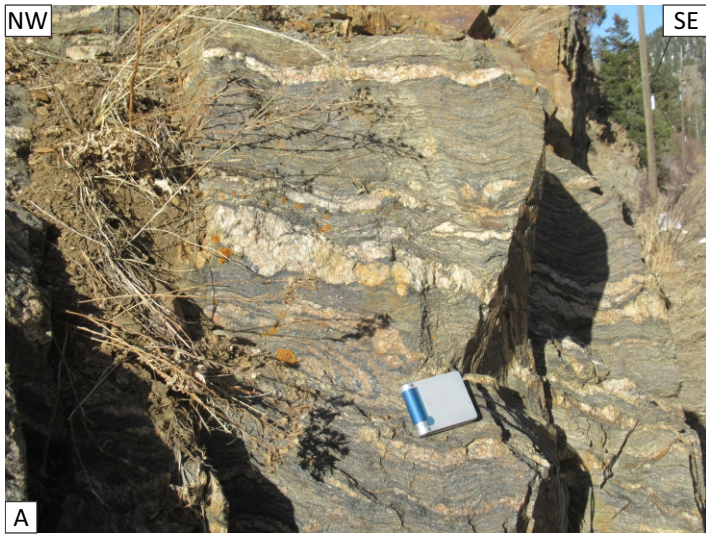


Figure 15